

Overview of JET Results

J.Pamela 1), J.Ongena 1,2) and EFDA-JET collaborators

1) EFDA JET-Close Support Unit, Culham Science Centre, Abingdon, Oxon, OX14 3EA
 2) LPP/ERM-KMS, Association EURATOM-Belgian State, B-1000 Brussels, Belgium

Email : jef.ongena@jet.efda.org

Abstract

High density and high confinement operation in ELMy H-Mode is confirmed at or above the normalised parameters foreseen for the ITER operating point ($H \sim 1$, $n/n_{GW} \sim 1$, $\beta_N > 1.8$ at $q_{95} \sim 3$). The scaling of the ELMy H-Mode with β_N could be more favourable than predicted by the IPB98(y,2) scaling. In ELMy H-mode, ICCD control of large sawteeth stabilised by fast particle has been demonstrated and the underlying NTM and sawtooth physics is being refined. At high-density type-I ELMy H-modes show trends that would lead to marginally acceptable ELMs on ITER. Type II ELM regime has been produced, but under very restrictive conditions. Type III ELMy operation with radiation fractions up to 95% has been demonstrated by seeding of N_2 in H-modes and could extrapolate to $Q=10$ ITER operation, albeit at high current (17 MA). The mitigation of Type-I ELMs nevertheless remains a challenge. Considerable progress has been obtained in ITB plasmas, with operation at central densities close the Greenwald density or/and low toroidal rotation or/and high triangularity. Full CD demonstration and successful simultaneous real time control of safety factor and temperature profiles have been achieved in ITB plasmas. RWM physics have been compared with theory, showing favourable scaling to ITER. High $\beta_N \sim 2.8$ operation of hybrid modes (also called improved H-modes) has been obtained with dominant NB. Hybrid modes with dominant RF heating have also been achieved. Trace Tritium Experiments yielded valuable information on particle transport in H-mode, ITB and hybrid regimes. In Type I ELMy plasmas, successful tests of the conjugate-T ICRF scheme have been achieved as well as LHCD coupling at ITER-relevant 10-11cm distances. Reduced D and T fuel retention has been observed, which could relate to operation with vertical targets in the divertor and/or lower (ITER-like) vessel temperature. It is confirmed that erosion occurs predominantly on the main chamber surfaces, with possible benefits for T retention in ITER, although consequences for the metallic first wall lifetime need to be assessed. Disruption and ELM studies indicate that transient power deposition could be less constraining than expected for the ITER divertor, but more challenging for the metallic first wall. Alpha particle tomography and direct observation of alpha particle slowing down have been made possible by γ -spectroscopy. Measurements of Alfvén cascades have been improved by a new interferometric technique. Promising tests of ITER relevant neutron counting detectors have been conducted.

1. Introduction

JET's technical capabilities (major radius of 3m, plasma current up to 5 MA in the present divertor configuration, ITER-relevant plasma triangularities, tritium operation and use of beryllium) allow plasma physics studies in conditions very close to those of burning plasmas. JET therefore provides key contributions in preparation of ITER operation, in particular: (1) the ELMy H-Mode and Advanced Tokamak regimes foreseen to be used on ITER are further developed and their scaling as well as underlying physics studied in an as relevant as possible (ρ^* , v^* , β_N) range; (2) significant progress is made on burning plasma physics; (3) ITER-relevant diagnostic and heating techniques are being tested.

A specific characteristic of the period 2003-2004 is that the scientific progress in preparation of ITER benefited from a reinforcement of coordinated experimentation between tokamaks worldwide, in particular between large and middle-size D-shape tokamaks. This period has therefore seen an unprecedented number of similarity and identity experiments involving two or more tokamaks, as well as coordinated parametric scans. Several of the results presented below result from such scientific co-operation.

During the past two years the use of JET was very intensive, with 165 days of experimentation. Of these, a total of 115 days were devoted to pure D plasmas in standard conditions for plasma current and toroidal magnetic field, 10 days for experiments with reversed plasma current and toroidal field in D plasmas, 20 days for studies in H and ^4He plasmas and 20 days for a dedicated Trace Tritium Experiment (TTE), mainly devoted to transport and particle confinement studies. This was the third time that Tritium was used on JET, after the PTE experiment in 1991 and the DTE1 in 1997. The removal of the septum in the divertor provided additional flexibility in plasma configurations (Fig. 1). Furthermore, the experiments on JET benefited from technological developments in control, heating and diagnostic systems.

Progress in preparation of ITER operating plasma scenarios is summarised in Sections 2 (performance), 3 (physics understanding) and 4 (real time control). Burning plasma physics results are presented in Section 5. The large size and plasma current of JET allow the effects of large disruptions and ELMs to be studied; in particular key issues in preparation of ITER operation are addressed, such as power deposition, erosion, sputtering and forces on first wall and divertor elements, with results reported in Section 6. Progress reached in the physics of ICRF heating and in ICRF and LH coupling are reported in Section 7. The increasingly demanding experimental conditions and requirements on the quality of measurements constitute a strong driver for diagnostics development, with progress presented in Section 8, particularly emphasising burning plasma diagnostics. Only a concise selection of the results obtained during the TTE Campaign (See Sections 3, 5, 7 and 8) is contained in this paper since a detailed overview is presented in another paper to this conference [D.Stork et al., this conf.]. More details on all the topics covered can be found in the various contributions of JET to this conference.

2. Performance of ITER operating scenarios

The ITER baseline scenario which is presently foreseen for reaching a power amplification $Q=10$ is the ELMy H-mode. Consolidation of this operational scenario has made continued progress, aiming at refining the fusion performance prediction and finding ways to reach higher fusion performance on ITER. Results are presented in Section 2.1 and in Section 3. Obtaining tolerable ELMs in this scenario remains a high priority topic. ELMs and other phenomena are discussed in Section 6.

The benefit of having steady state (or near-steady state) operations in a future tokamak fusion reactor has also triggered efforts toward the development of the so called Advanced Tokamak (AT) regimes, which would allow for a large fraction of non inductively driven current. Advanced Tokamak (AT) regimes discussed in this paper cover the purely non-inductive ‘steady-state’ mode of operation, characterised by a reversed q profile ($q_0=2-3$, $q_{min}=1.5-2.5$), and by the presence of an Internal Transport Barrier (ITB) and the ‘hybrid’ regime ($q_0>1$, $q_{95}\sim 4$, monotonic q profile, also called improved H-mode), which is an intermediate scenario between the inductive H-mode and the fully non-inductive current drive regime operating scenario. The results on ITB plasmas are mainly reported in Sections 2.2, 3 and 4, and those related to the hybrid mode in Section 2.3 and 3.

2.1 ELMy H-Mode Performance

High density high confinement operation. The ELMy H-Mode is the reference operating scenario for ITER, projected to deliver a power amplification by fusion reactions $Q=10$. Although the realization of this scenario at values for q_{95} , β_N , n/n_{GW} , $H_{98(y,2)}$ and δ at the ITER working point has been demonstrated in the last years on JET, optimisation continues, in particular in boosting further the performance in confinement and density, and in documenting better the scaling of energy and particle confinement and the threshold power for the L-H transition. ELMy H-mode plasmas at ITER-like triangularities ($\delta_{av}=0.47$) have been obtained at $H_{98(y,2)}=1$, $n/n_{GW}>0.85$, $\beta_N=1.8$ for plasma currents up to 2.5 MA ($q_{95}=3.0$) and for $I_p=2.5-3.5$ MA ($q_{95}=3.0$), at somewhat lower $\delta_{av}=0.42$, with $\beta_N=1.6-2.0$. ELMy H-Mode plasmas simultaneously realising (or exceeding) the ITER values for q_{95} , β_N , n/n_{GW} , $H_{98(y,2)}$ reach $\rho^*/\rho^*_{ITER}=1.1-1.3$ but at relatively high $v^*/v^*_{ITER}=6-11$. Large NTMs were successfully avoided by implementing operational strategies, which prevent large sawteeth or first ELMs, both of which can trigger NTMs via large seed islands. At high densities ($n/n_{GW}\sim 1$) the H-mode pedestal enters the mixed Type I/II ELM regime, characterised by an increasing pedestal pressure caused by an increased pedestal density at roughly constant temperature, a decreasing Type I ELM frequency and increased inter ELM losses accompanied by enhanced low frequency magnetic fluctuations.

L-H Transition. Experiments were carried out on JET to study the effects of divertor geometry and plasma shaping on the power needed for the L-H transition, P_{L-H} . Plasma configurations run with the septum removed from the divertor (Septum Replacement Plate divertor - MkII-SRP - see Fig. 1), identical to configurations previously run in the Gas Box Divertor (MkII-GB) have shown that the presence of the septum lowers P_{L-H} by 20 %. This result can largely be explained by a constant pedestal T_e at the L-H transition both with and without the septum and the differences in power needed to reach it. Additional experiments show that with a lowered X-point height, plasmas run with the MkII-SRP divertor reproduce a significant decrease in P_{L-H} (up to a factor of two for a variation in X-point height of about 16cm) and pedestal electron temperature T_e , first observed with the MkII GB septum divertor. Experimental studies of plasma shaping effects have shown δ^{up} to have no influence on P_{L-H} or pedestal T_e/T_i . Attempts to study the influence of δ^{low} are so far inconclusive, as such variations require a variation in the X-point height. Finally, a comparison of the reversed B_t discharges with reference plasmas with the standard B_t direction shows no significant difference on P_{L-H} in JET, in contrast to ASDEX-Upgrade [W.Suttrop et al., PPCF 39 2051-2066(1997), F.Ryter et al., PPCF 40 725-729 (1998)] and DIII-D [T.Carlstrom et al., PPCF 40, 669-672 (1998)].

Deuterium only fuelling scans at $q_{95}=3.4$ have confirmed the Borrass-Lingertat-Schneider scaling [K.Borrass et al., NF 44, 752-760 (2004)] of the H to L back-transition density, irrespective of triangularity, suggesting that the intended Greenwald fraction in ITER would be inaccessible by gas injection alone. This could partially be offset by density peaking, since studies of Type III H-modes with mid-radius collisionality, brought within a factor of two of the ITER value, have indicated that the particle diffusivity was about 5 times lower than assumed in current modelling, with consequently moderate profile peaking. [H Weisen et al., this conf.]

2.2 Performance of Advanced Modes with Internal Transport Barriers

The closeness of the JET scenarios to those foreseen for ITER in terms of physics parameters (simultaneously ρ^* , v^* and edge conditions) allows detailed investigations of possible solutions to e.g. integrated Real Time Control (RTC) of AT regimes, their compatibility with low momentum input and ITB resilience to ELMs. During the 2003-2004 experimental Campaigns, the Advanced Tokamak studies on JET progressed significantly thanks to: (i) an enhanced RTC system, now allowing to control a multitude of signals on-line, with as highlight the simultaneous control of the pressure and q profile (See Section 4) [D.Moreau et al., this conf.], (ii) further progress in Lower Hybrid (LH) coupling (See Section 7) [J.Mailloux et al., this conf.], (iii) the increased plasma shaping capability deriving from the removal of the septum from the divertor (Fig. 1) and (iv) a further increase in the neutral beam heating power.

While the inductive H-mode is relatively well explored, an open issue is how the presently developed non-inductive current drive regimes with improved core confinement will extrapolate to next-step experiments. During the 2003-2004 experimental campaigns, the physics of improved core confinement regimes and the conditions for the formation and sustainment of AT regimes [A.Tuccillo, this conf.] have been further investigated. An extensive database [X. Litaudon, PPFC 46, (2004) A19-A34] on the advanced mode of operation has been assembled covering a wide range of plasma parameters (q -profile, T_i/T_e , R/L_T gradient length, triangularity, Larmor radius ρ^* ,

collisionality ν_e^* , Mach number M_Φ ...).

High density operation. Until recently, one of the main difficulties was the low target density ($n/n_{GW} < 0.5$) of AT discharges. ITBs on JET can now be triggered with core density close to or above the Greenwald density using an adequate timing of LH and pellet injection to reach a reversed q profile and peaked density profiles. Under these conditions, ITBs have been observed on the profiles of ion- and electron temperature, density and toroidal rotation and at a bulk plasma rotation 4 times lower than in ITB plasmas at low target density and high NBI input power. This has been obtained with simultaneous NBI (8-9MW) and ICRH (6-7MW) (JPN57941) heating leading to ITBs with $T_e \sim T_i \sim 7\text{keV}$. The foot of the ITB in this case is typically inside $R=3.5\text{m}$, i.e. inside mid-radius.

Large Internal Transport Barriers. Large ITBs ($R > 3.5\text{m}$) can be formed by reducing the magnetic shear close to a low order rational surface in the vicinity of the plasma boundary. This has been done in two different ways : (i) in the current ramp-up at high plasma current ($I_p/B_t \sim 3.0\text{MA}/3.2\text{T}$) and low q_{95} (~ 3) relying on the slow penetration of the off-axis ohmic current. At these high currents only low triangularity discharges could be explored up to now on JET (lower disruptive forces); (ii) at low plasma current ($I_p \leq 2\text{MA}$) and high q_{95} ($> \sim 5$) in the presence of a large fraction of off-axis driven current (LHCD and bootstrap current). The latter have been realised in both high and low triangularity discharges. At low triangularity, the ITBs are located at $R=3.6\text{m}$, close to $q=3$ surface, generally do not accumulate impurities (due to the weaker density and temperature gradients at the obtained high radii of the ITB) and can coexist with another internal barrier (ITB located at $R \sim 3.3\text{m}$), in a zone with strong negative shear. These discharges show type-III ELMs and are reproducibly sustained for a time close to neo-classical resistive time ($\sim 10\text{s}$).

The largest ITBs ($R \sim 3.7\text{m}$) have been found at high triangularity $\delta \sim 0.45$ in $3.4\text{T}/1.5\text{MA}$ at $q_{95} \sim 7.5$ plasmas with combined NBI = 18.5MW, ICRH = 2.5MW and LH = 2MW (JPN62293) heating. [Rimini this conference]. At large triangularity the main difficulty is to optimise simultaneously the edge conditions (avoiding type I ELMs) and q -profile to maintain the barrier. Despite the closeness of foot of the barrier to the edge pressure pedestal, type I ELMs can be moderated using Ne seeding. The performance reached with this scenario is as follows: $\beta_p = 1.5$, $H_{89} = 1 \sim 1.8$, $\beta_N \sim 1.8$, $n/n_{GW} \sim 70\%$, $P_{\text{rad}}/P_{\text{tot}} \sim 50\%$ and $V_{\text{loop}} \sim 0.05\text{V}$.

Long Pulse Operation. Highly non-inductive reversed shear operations have been achieved in $3\text{T}/1.8\text{MA}$ discharges where a combination of 10MW NBI, 5MW ICRH and 3MW LH power is applied. These pulses have been optimised at reduced NBI power such that the power delivered by each beam box could be applied sequentially in time. At low beam power, the peak performance is reduced to $H_{89} = 2$, $\beta_N \sim 1.66$ and with a bootstrap fraction of about 33%. In these conditions the pulse duration has been extended to the maximum duration allowed by the JET subsystems ($20\text{s} \sim 2 \times \tau_{\text{res}}$) with a record of injected energy $E \sim 326\text{MJ}$.

ITB formation. In order to investigate the physics and extrapolation of the ITB formation in terms of non-dimensional parameters identity experiments between JET and ASDEX-Upgrade have been undertaken at similar q -profile (i.e same $q_0 \sim 2$, q_{95} and shape), ρ^* , ν^* . A similar phenomenology of the ITB formation and erosion due to Type I ELMs has been reproduced on JET. Moreover on JET, the ITB regime, transient on AUG, has been sustained on longer time scales ($10 \times \tau_E$) with barriers present both on ion- and electron temperature profiles through the mitigation of ELMs by Ne injection.

2.3 Development of Hybrid Modes

Identity experiments have been also performed between JET and ASDEX-Upgrade to confirm the existence of the hybrid regime closer to ITER parameters (Joffrin, IAEA). JET experiments first focused on reproducing the hybrid regime with a careful match of the magnetic configuration, q profile, ρ^* and plasma β with those of ASDEX Upgrade hybrid plasmas. The performance of hybrid scenario plasmas on JET has been successfully verified up to $\beta_N = 2.8$ at low $B_t = 1.7\text{T}$ and $I_p = 1.4\text{MA}$, at both high and low plasma triangularity ($\delta = 0.2$ and 0.45) and ρ^* corresponding to the ASDEX Upgrade discharges. Stationary conditions have been achieved with a figure of merit for fusion gain $H_{89} \cdot \beta_N / q_{95}^2$ reaching 0.42 at $q_{95} = 3.9$ at a Greenwald density fraction of 0.7 , equivalent with $\nu_e^* \sim 0.08$ or $4 \times \nu_{e, \text{ITER}}^*$.

Dedicated similarity experiments have then extended the hybrid regime operations on JET to lower ρ^* (as low as $\rho^* = 3.3 \cdot 10^{-3}$ or $2 \times \rho_{\text{ITER}}^*$ and $\nu_e^* \sim 0.06$ or $3 \times \nu_{e, \text{ITER}}^*$) by increasing the toroidal field ($B_t = 2.4\text{T}$ and 3.1T). The operation at high current and field (necessary to keep both ρ^* and ν^* simultaneously closer to ITER) has yet been restricted to lower β_N values due to limited heating power (Fig.2) The parametric range needs to be extended to values closer to the ITER values to allow a full set of scaling studies.

This regime has also been reproduced at low plasma rotation with dominant RF heating (NBI = 7.8MW, LH = 1.2MW, ICRH = 10MW) in plasmas with $I_p/B_t = 2.6\text{MA}/3.2\text{T}$, $q_{95} = 3.8$ (JPN62789), resulting in $q_0 \sim 1$, T_i close to T_e , $H_{89} = 2$, $\beta_N = 1.55$ with Type III ELMs [C.Gormezano et al., EPS 2004]. Up to now no impurity accumulation has been seen in the hybrid regime.

The special importance of the hybrid mode is the avoidance of mechanisms of triggering deleterious NTMs by sawteeth ($q_0 > 1$). This provides the possibility of extending this mode towards high β_N operation. In JET, the hybrid regime has been operated with small NTM islands (2-3cm) up to high value of β_N (~ 2.8) reaching more than 90% of the ideal kink limit. In these discharges the β_N values approach the no wall limit defined empirically by $\beta_N \sim 4I_i$. Operation above this limit requires higher additional heating power.

3. Physics studies related to fusion performance of ITER-relevant plasma scenarios

3.1 H-mode Confinement Scaling

The scaling of energy and particle transport for ELMy H-Modes, in terms of non-dimensional parameters, has been studied with a series of ρ^* , β and ν^* scans. Tritium particle confinement was studied with trace tritium

($n_T/n_D < 5\%$) puffing and beam blips into a low $q_9 = 2.8$, low triangularity $\delta = 0.2$ D plasma. Energy confinement was studied in pure D plasmas.

Two ρ^* scans for energy confinement were performed in the same scenario with both Type I ($\beta_i = 2.6\%$, $I_p = 2.4$ MA) and Type III ($\beta_i = 1.3\%$, $I_p = 1.3$ – 4.3 MA) ELMy H-mode plasmas. A gyro-Bohm like scaling was found for both the Type I ($\omega_{ci}\tau_E \propto \rho^{*3.2 \pm 0.4}$) and Type III ($\omega_{ci}\tau_E \propto \rho^{*-2.9 \pm 0.5}$) scans, consistent with that seen in IPB98(y,2). A three point ρ^* scan for tritium particle confinement showed a similar gyro-Bohm like dependence ($D_T/B_0 \propto \rho^{*3.2 \pm 0.6}$) for $0 < r/a < 0.45$, but with a weaker Bohm-like dependence in the outer region ($D_T/B_0 \propto \rho^{*1.9 \pm 0.4}$) ($0.65 < r/a < 0.85$).

Two two-point β scans for energy confinement were also performed in the same scenario, along with a three-point β scan in higher q ($q_9 = 3.2$) and triangularity ($\delta = 0.3$) plasmas. In contrast to the IPB98(y,2) scaling, a very weak beta dependence ($\omega_{ci}\tau_E \propto \beta^{-b}$, with $b = -0.03$ to $+0.04$) was found for energy confinement in the three scans, confirmed in complementary experiments on DIII-D [C. C. Petty et al., Phys. Plasmas **11** (2004) 2514], consistent with transport dominated by electrostatic processes and in agreement with previous dedicated scans [J. P. Christiansen et al., NF **38** (1998) 1757; C.C. Petty et al., NF **38** (1998) 1183]. The two point β scan for tritium particle confinement, by contrast, showed a positive impact of β on particle confinement ($D_T/B_0 \propto \beta^b$, with $b = -0.34$ to -0.55) which contradicts IPB98(y,2). A model, based on neoclassical orbits in stochastic electromagnetic fields [I. Voitsekhovitch et al., Phys. Plasmas, in prep.], has been shown to reproduce the observed beta dependence of particle confinement, but a unified model, describing the β dependence of particle and energy transport, remains outstanding.

A v^* scan in a $q_9 = 4.4$, $\delta = 0.4$ scenario, showed energy confinement having a negative dependence on v^* ($\omega_{ci}\tau_E \propto v^{*-0.35 \pm 0.04}$), in contrast to the negligible ($\omega_{ci}\tau_E \propto v^{*-0.01}$) IPB98(y,2) scaling. These new findings support electrostatic energy confinement scalings, which predict a moderate increase in energy confinement ($\Delta\tau_E/\tau_E = 2$ – 28% , depending on the details of the scalings used) for the ITER $n/n_{GW} = 0.85$, $\beta_N = 1.8$ baseline, but a dramatic increase at higher β_N ($\Delta\tau_E/\tau_E = 23$ – 50% for $\beta_N = 3.0$), which would allow operation with fusion gains of $Q > 15$ at $n/n_{GW} = 0.85$ and even higher values, $Q > 20$, for $n/n_{GW} \approx 1.0$. (Fig. 3)

Dimensionless identity experiments have been jointly conducted on JT60-U and JET, aimed at the comparison of the H-mode pedestal and ELM behaviour [G. Saibene et al., this conf.]. Differences have been observed in the pedestal characteristics, and dedicated experiments have shown that these are related to ripple induced fast ion losses in JT60-U. Physics mechanisms relating ripple losses to pedestal performance are not yet identified. The role of velocity shear in the pedestal MHD stability, as well as the possible influence of ripple on thermal ion transport, are under investigation.

3.2 Particle Transport Experiments during the Trace Tritium Campaign [K.-D. Zastrow et al, this conf.]

The JET Trace Tritium Experimental (TTE) campaign used deuterium plasmas with trace amounts of tritium (T) ($n_T/n_D < 3\%$) to investigate thermal fuel-ion transport, fast particle dynamics and heating and current drive physics [D. Stork et al., this conf.]. The non-dimensional parameters ρ^* , v^* and q_9 were varied in pairs of sawtoothed ELMy H-Mode discharges, to compare the scaling for the transport coefficients of fuel particles. The main results can be summarised as follows. Tritium particle transport is generally above neoclassical levels (as calculated by NCLASS [W. Houlberg, Phys. Plasmas, **4** (1997) 3230]) and only under two circumstances are neoclassical values approached: at high density in high current, low q_9 discharges [P. Belo et al., EPS 2004] and in the transport barrier region of ITB discharges [J. Mailloux et al., EPS 2004]. In hybrid scenarios τ_{pT} improved by $\sim 50\%$ in triangularity scans ($\delta = 0.2$ – 0.46) at constant energy confinement. Comparing different regimes (ELMy H-mode, ITB plasma, and Hybrid scenarios) outside the central plasma region ($0.65 < r/a < 0.85$), the tritium diffusion coefficient (D_T/B_ϕ) scaling is consistent with Gyro-Bohm ($\sim \rho_\theta^3$, where $\rho_\theta^* \propto q\rho^*$), but with an inverse β dependence, in contrast to energy transport which shows no dependence on β as reported in Section 3.1. The impact of the unfavourable increase of particle confinement on ITER operation at high β_N remains to be assessed. [D. McDonald et al, this conf.].

3.3 Transport Physics and Tests of Theoretical Models

Theory predicts that both thermo-diffusion and magnetic field curvature contribute to the turbulent pinch [X. Garbet et al., PRL, **91**, 035001/1-4]. Also curvature pinch depends on magnetic shear and the peaking factor decreases with collisionality. These predictions have been tested against experimental results at JET. It has been verified that the pinch velocity increases with magnetic shear in L-mode plasmas [L. Garzotti et al., NF **43**, 1829 (2003), H. Weisen et al., PPCF **46** (2004) 751]. In H-mode, the density peaking is sensitive to collisionality, consistently with ASDEX-Upgrade results. It is found that at high collisionality, the pinch velocity is close to the Ware value, whereas it is larger at low collisionality [H. Weisen et al., PPCF, submitted; M. Valovic et al., PPCF, in print]. This suggests that density profiles in ITER may be more peaked than presently assumed. RF heating is found to flatten density profiles. When collisionality is large, this is interpreted as an increase of the turbulent diffusion coefficient driven by ion heating while the pinch velocity stays close to the neoclassical value. For low-density plasmas, the interpretation rather relies on electron heating inducing the weakening (and may be reversal) of pinch velocity predicted by theory when the turbulence moves from ion to electron dominant instabilities. For these reasons, it is believed that alpha particle electron heating in ITER (where ion instabilities will still be dominant) will not have a dramatic flattening effect on density profiles. RF heating was also found beneficial to control impurity accumulation via a decrease of impurity inward convection [M. E. Puiatti et al., PPCF **44** (2002) 1863], although it is still not clear if the effect is due to a reduction of the neoclassical impurity pinch associated to density flattening or to a modification of the significant turbulence driven component of impurity convection.

Heat modulation experiments have been undertaken at JET using ICRH in mode conversion scheme. These experiments have been analysed using a critical gradient transport model, stability analysis and predictive

modelling. Instability thresholds are found to be in the expected range for micro-instabilities in tokamaks. Electron stiffness was found to cover an unexpectedly wide range of variation [X. Garbet et al., PPCF **46**, 1351 (2004)]. However the Weiland transport model was able to reproduce experimental results [P. Mantica et al., EPS 2004]. A correlation was found between electron stiffness and the ion temperature gradient length [P. Mantica et al., this conf.]. This observation suggests that some interplay exists between electron and ion heat channels. The applicability of a critical gradient model in the case where ion and electron modes are linearly unstable will thus have to be further investigated. No firm conclusion can yet be drawn regarding profile stiffness in ITER.

3.4 Resistive Wall Modes and High Beta Operation of Advanced Modes

In advanced tokamak operating scenarios, such as those foreseen for ITER and compatible with the steady-state operation of a power plant, the ultimate performance limit is set by resistive wall modes (RWMs) [Liu Y Q et al, NF **44** (2004) 232]. Therefore, the RWM must be stabilised in order to achieve steady state operation with high plasma pressures. The RWM is a kink mode whose growth rate is largely governed by the tokamak wall time but whose stability is related to damping depending on the velocity of plasma rotation. Calculations using MARS-F code [Liu Y.Q., et al., Phys. Plasmas **7** (2000) 3681] show that the critical rotation required for RWM stabilisation depends sensitively on the damping models.

The damping of stable RWMs may be determined experimentally by measuring the response to $n=1$ helical magnetic perturbations from coils external to the plasma - in JET, saddle coil systems both internal and external to the vacuum vessel have been used for such studies [T C Hender et al, this conf.] and then compared with the MARS-F predictions. The resonant field amplification (RFA) of this externally applied field has been measured for both DC and AC applied magnetic perturbations. RFA was observed as β increases, particularly beyond the no-wall limit, and comparison with MARS-F modelling shows agreement [Liu Y.Q., et al., Phys. Plasmas **7** (2000) 3681] with experiment. The occurrence of a critical flow velocity below which the RWM becomes unstable was found to be in agreement with modelling [Y Liu et al, this conf.].

The results of these first European experiments on resistive wall modes in tokamak plasmas provide a very important experimental validation of RWM damping models allowing for extrapolation to ITER, and it is found that the observed strong damping leads to a requirement for a flow of ~ 2 to 3% of the Alfvén velocity at the plasma centre to stabilise the RWM. It is marginal whether the flow velocity in ITER will reach such values indicating that an active RWM control system will be a prudent option.

4. Real Time Control of ITER operating scenarios

Real-time control of the reference scenarios for ITER is of key importance. Two examples will illustrate this. For the ELMy H-Mode, where the plasma shape is a main element in determining the performance, high triangularity and elongation need to be maintained during the pulse, even in the presence of (large) variations of current or pressure profile. For Advanced Modes, the q-profile plays a crucial role in accessing high confinement, stability and current drive, and controlling its shape is therefore a key element in establishing and maintaining high performance.

4.1 Control of the plasma shape

A control system that is able to maintain the plasma shape in presence of large disturbances (e.g giant ELMs and large variations of β_p and/or I_i) is a key element for performing successful experiments. The eXtreme Shape Controller (XSC) system has been successfully installed and commissioned during a recent experimental campaign on JET. The description of the plasma shape is done with a set of geometrical descriptors (gaps), that define the distance along predefined directions of the last closed flux surface from the first wall. In order to control the overall plasma shape during a JET pulse, the XSC has been designed to implement a system in which all 8 poloidal coils are used as actuators for the real-time control of a large set of geometrical descriptors (48). Since the number of available actuators is only 8, an optimisation process that defines the sensitivity of each gap to a variation of the current of a given coil has been performed by means of a singular value decomposition (SVD) analysis. The design aims have been demonstrated during a set of high triangularity ITBs discharges in presence of quite large variations of β_p (β_p up to 1.5) and/or I_i (I_i up to 0.5) [F.Sartori et al, SOFT 2004].

4.2 Control of plasma profiles in Advanced Tokamak Regimes

To sustain ITBs on ITER time scales, a careful optimisation of plasma characteristics and power tailoring through integrated Real Time Control of ITB strength and profiles will be required. E.g. the presence and size of a 'current hole' in discharges with deep reversed shear should be carefully controlled during the high D-T fusion yield phase of future experiments, since (i) these configurations are characterised by a low confinement of fusion born alphas as measured during TTE [V.Yavorskij et al., NF **43** (2003) 1077].and (ii) deleterious TAE modes could be triggered with large values of q_{95} . Past experiments [D.Mazon, PPCF **45** (2003) L47-L54] focussed on the separate control of the maximum normalised electron temperature gradient ρ^*_{Te} or the safety factor profile in different discharges. A major challenge still remained to simultaneously control both the current and pressure profiles, which mix up the resistive and confinement time scales in a non-linear way. Multi-variable model-based techniques [L.Laborde et al., EFDA-JET Preprint EFDA-P(04) 28; Moreau et al., this conference] for the control of the current and/or the pressure have now been developed. The technique aims at minimising an integral square error signal that combines the two profiles, rather than attempting to control plasma parameters at some given radii with great precision. The resulting flexibility of the control scheme allows the plasma to relax towards a physically accessible non-linear state which may not be accurately known in advance, but is close enough to the requested one to provide the required plasma performance. Closed loop experiments have allowed to satisfactorily reach different

target q and ρ^*_{Te} profiles, and, to some degree, to displace the region of maximum electron temperature gradient. The control has also shown some robustness in front of rapid transient events like Type I ELMs, and spontaneous emergence or collapses of the ITBs. An improvement of the proposed technique could consist in identifying a dynamical linear model which would allow to design a two-time-scale controller, perhaps more suited to control rapid plasma events while slowly converging towards a requested steady state.

4.3 Control of impurity content, confinement and density

A dual feedback system was developed in order to control both the values of $H_{98(y,2)}$ and $\gamma = P_{rad}/P_{tot}$. The D_2 puffing rate and the Ar seeding rate are used as actuators. Confinement and radiation were chosen as controlled parameters since they were the best correlated quantities with the actuators. Furthermore this choice allows to maximise the D_2 fuelling rate for a given confinement and radiation. The feedback scheme uses a 2 by 2 control matrix, which is established from open-loop experiments with step requests for the actuators and is valid for a certain range around the chosen operational point, which results from the strong non-linear couplings between the various physical quantities to be controlled. The plasma model – essentially described by this matrix – is then tested on several discharges from the existing database. Once the plasma model is responding satisfactorily it is implemented in the feedback loop in order to test the stability of the scheme and optimise the Proportional, Integrated and Differential (PID) time constants of the loop. This procedure has been successfully applied to Ar seeded discharges, showing simultaneously high confinement and high density (See Section 6.4) for the whole feedback control phase ($>5s$) [P.Dumortier et al., EPS 2004]

5. Burning Plasma Physics [Stork et al., this conf.]

5.1 Confinement of alpha particles in ELMy H-Mode and Current Hole discharges

Alpha particle confinement in ELMy H-Mode and Current-Hole (CH) plasmas, was studied [V. Kiptily Phys.Rev.Lett, S.Sharapov, this conf.] by detecting γ -rays from reactions between fusion alphas (generated by Tritium Neutral Beam blips, TNB) and beryllium impurities ($^9Be(\alpha, n\gamma)^{12}C$) in deuterium plasmas after TNB turn-off. γ -ray emission decay times measured the fusion- α population slowing-down time (τ_{as}). In CH discharges τ_{as} determined in this way was ~ 5 times lower than classical values (Fig. 4), indicating α -confinement degradation, due to orbit losses as predicted by 3-D Fokker Planck code. Studies in ELMy H-Mode plasmas confirmed the classical picture of the alpha particle slowing down. [V.Yavorskij et al., NF 43 (2003) 1077].

5.2 Fast ion dynamics

Fast ion confinement and instabilities (Toroidal Alfvén Eigenmodes (TAEs), Alfvén Cascades (ACs)) are key elements in determining the plasma heating, fast ion dynamics and transport in next-step burning plasma devices such as ITER. Several different groups of fast ions will be present in such a machine (4He , D, 3He and H resulting from fusion reactions, MeV range injected beam ions and ICRH-accelerated ions) and it is essential to measure and understand the consequences of transport and instabilities for each group of fast ions separately. These issues have been addressed in experiments on JET, with innovative diagnostic techniques, in conventional and shear-reversed plasmas, exploring a wide range of effects.

Fast alpha tails have been successfully created in both H-mode and reversed shear scenarios during the He campaign using third harmonic ICRF acceleration of 4He beam ions in 4He plasmas [S. Sharapov et al., this conf.; M.Mantsinen et al., *Energetic Particles in Magnetic Confinement Systems*, (Gothenburg, 2001), Vol. OT-28, IAEA]. The plasmas consisted of a mixture of D and 4He with $n_D/n_{He} = 10/90$ and $B_t = 2.2$ T. The value for B_t was determined by the need for on-axis ICRF-heating of the 4He beam, and by the presence of two hydrogen resonances at the inner and outer walls of the machine. have been created in a ‘D-T neutron-free’ environment. Simultaneous measurements of spatial profiles for fast Deuterium and alpha particles were performed successfully for the first time with gamma-ray tomography (See Section 8.2), confirming agreement of fast particle dynamics with the classical theory of fast ion orbits in plasmas with monotonic and strongly reversed magnetic shear.

In ELMy H-mode plasmas (JPN 54165) a 4He tail temperature of $T_{fast} \sim 1.1 \pm 0.4$ MeV [M. Mantsinen et al., PRL, 88 (2002) 105002] with a density of fast 4He ions up to $n_{fast}/n_e \sim 10^{-3}$ was obtained, very close to fusion alpha temperatures and densities observed ($T_{fast} \sim 1$ MeV and $n_{fast}/n_e \sim 4 \cdot 10^{-3}$) in the JET record DT fusion H-mode discharge (JPN42976) [M.Keilhacker et al., NF 39 (1999) 209], but at negligibly small neutron rate, R_n (JPN54165) $\leq 10^{14} s^{-1} \ll R_n$ (JPN42976) $\approx 5.7 \cdot 10^{18} s^{-1}$. The acceleration technique has also been applied to strong shear-reversed plasmas with full NBI power (JPN63047 and 63048) and yielded results on alpha particle orbits in current hole discharges (Section 5.1).

Differences with fusion alphas in a real D-T pulse are: (i) the anisotropy of the fast ion distribution function in a relatively cold plasma and (ii) the absence of self-consistent profiles of fast and thermal ions. However, this scenario allows the investigation of some aspects of alpha particle physics, such as orbit losses and thermal plasma heating by fast 4He , without expensive DT operation. It also allows the development and testing of alpha particle diagnostics in a non-contaminated environment at low neutron yield. Future experiments are being considered at higher magnetic field.

With ICRF minority heating of 3He (in 4He plasmas) and H (in D plasmas) tails of fast 3He and H were created. Direct profile measurements of the created fast ions were also performed using gamma-ray detection (see Section 8.2). Time-resolved measurements of fast 3He profiles were performed with a time resolution up to 10 ms (which is possible due to the high intensity of the gamma radiation for the reactions considered), while the energy spectrum was measured with a gamma-ray spectrometer and a neutral particle analyser. Numerous Alfvén eigenmodes: TAEs, EAEs, Alfvén Cascades have been excited in these experiments. However, no notable

degradation of the fast ion confinement or losses was observed in these discharges with relatively small fast ion orbits, $\Delta_{\text{fast}} \sim 0.1 a$, as compared to the minor radius a . In the opposite case of large drift orbits, $\Delta_{\text{fast}} \leq 0.5 a$, obtained for 5 MeV ICRH-accelerated protons, a strong coupling between Alfvén modes inside and outside the $q=1$ surface was observed in plasmas with a flat and monotonic q profile, and a significant degradation of fast proton confinement was observed during the TAE-activity on gamma-ray diagnostics.

Evolution of beam ions due to fishbones and TAEs excited by NBI with $V_{||\text{beam}} \sim V_A$ at low $B_t/I_p = 0.86 \text{ T}/0.9 \text{ MA}$ was investigated during the TTE. [S.Sharapov et al., EPS 2004]. 5.5 MW of D-NBI neutrals with $V_{||\text{beam}} \approx 0.73 V_A$ was injected leading to a destabilisation of TAEs/fishbones. T-NBI blips were added on top of the D-NBI and the temporal behaviour of the DT neutron profile was measured and compared with the TRANSP code modelling based on classical Coulomb collisions. A marked departure was observed of the measured DT neutron profile from TRANSP in discharges with fishbones, with the central region of the plasma inside $q=1$ being the most affected

5.3 Alfvén wave excitation studies

Experiments have shown the importance of edge magnetic shear, elongation and triangularity in determining the damping rate of low- n TAE modes. and the dependence of the damping rate on the bulk plasma beta and normalised Larmor radius been determined. Effects have been observed of rotation shear, q_0 and direction of the ion B-drift, on the damping rate of $n=1$ TAEs. New high- n TAE antennas are planned for installation on JET in 2005. These antennas will be devoted to exciting and detecting AEs with toroidal mode numbers 5-15, which are predicted to be the most unstable for ITER.

5.4 Control of Fast Particle induced Sawteeth

Alpha particles are likely to stabilise sawteeth in machines with strong central fusion heating. Seed islands appearing after the crash of such sawteeth tend to destabilise NTMs leading to a strong degradation of the confinement time. Localised current drive near the $q=1$ surface can destabilise sawteeth and the smaller crashes of sawteeth with shorter sawtooth periods do not lead to those detrimental effects. To show clearly the capability of ICRF to destabilise large sawteeth stabilised by fast particles, large sawteeth were first created and then destabilised. ICRF power of 3 MW in the (H)D minority scenario with a concentration of $n_H/n_D \sim 5\%$ and central resonance using a co-current directed (inward pinch of fast particles) spectrum efficiently created long sawteeth with a period of up to 250 ms in 2.6 MA plasma discharges. A power of 3 MW in counter-current propagating ICRF waves at the $q=1$ surface on the high field side decreased the sawtooth period to 80ms [Eriksson L.-G. et al., PRL **92** (2004) 235004-1 to 4]. The method is sensitive to the correct positioning of the resonance layer to within 5 cm.

6. Divertor and First Wall Studies in Preparation of ITER

6.1 Erosion and co-deposition at first wall components.

Material erosion, its subsequent transport in the plasma and final co-deposition with the plasma fuel is an important issue for operation with longer pulses of next generation devices. An idea of the scale of the problem can be seen by considering that a single ITER pulse is equivalent to half a year of JET operation in energy input (~ 1500 pulses) and about 5 JET years of divertor ion fluence (~ 15000 pulses).

Recent analysis through a variety of independent approaches has shown remarkable agreement between estimated rates of carbon impurity evolution from main chamber sources and inner divertor deposition. This provides strong support for an emerging view in the tokamak community that erosion occurs predominantly on main chamber surfaces (via charge-exchange neutral or ion impact) and that the resulting impurities are convected preferentially to the inner divertor during operation with the normal toroidal field direction (ion $B \times \nabla B$ drift downwards). Such preferential deposition has been directly confirmed on JET using dedicated $C_{13}H_4$ gas injection studies [J.Likonen et al., Fusion Engin. and Design, **66-68**, 219 (2003)] and through the use, unique to JET of beryllium evaporation in the main chamber. Strong parallel flows with Mach numbers between 0.2 and 0.6 have been measured near the top of the machine, directed from outer to inner divertor for normal field and are a clear candidate for the source of convective, long-range material transport. Considerable simulation efforts using both the EDGE2D-Nimbus [A.V.Chankin et al., J.Nucl. Mater., **290-293**, 518-524 (2001) and B2.5-Eirene code [D.Coster et al., paper P1-8, PSI 2004] packages are underway, though the measured flows remain anomalously high compared with numerical predictions when classical drift terms are included. A recent unexpected and unique finding has been that the outer divertor, normally a region of net erosion in JET, becomes a zone of net deposition following toroidal field reversal [R.A.Pitts et al., invited paper I-7, PSI 2004; J.Nucl.Mater., in press.]. This is accompanied by the observation of stagnant SOL flow in the main SOL and has added further importance to the code simulation efforts including drift physics. Whenever carbon is present (as in JET), however, the situation is complicated by plasma chemistry and a complete description of the erosion-redeposition process and subsequent short-range carbon transport is also needed. [V. Philipps et al., this conf.].

6.2 Tritium retention

Ongoing ex-situ analysis of graphite tiles from a whole series of previous JET divertors is revealing average fuel retention rates of $\sim 3\%$. For example, during the MKII-GB divertor phase, about 766g of deuterium fuel was injected and 22g found in the divertor following post-mortem tile analysis. This should be compared with the results of tritium balance during the JET DTE1 campaign in which 10.5% T retention was obtained after an extensive clean-up campaign. Recent in-situ measurements of material accumulation in remote areas indicates that

this overall reduction in retention may largely be due to regular operation in recent years with vertical target configurations in the gas box divertors compared with the earlier horizontal target operation, implying an important role for divertor geometry in determining the extent of migration and retention [V.Philipps et al., this conf.]. A very recent gas balance experiment in JET [T.Loarer et al., this conf.] in which ~40 reproducible, H-mode discharges with high fuelling were executed over a full day of operation showed essentially zero long term retention within measurement accuracy.

Following reprocessing of all T released from the torus during and after the TTE experiment, the T inventory indicated a full recovery of all T used for the experiment, indicating a very low T retention.

6.3 Disruption studies

Considerable effort has been devoted on JET towards improving both the database and understanding of energy and particle transients and the resulting transport to first wall surfaces. Analysis of energy flows from the bulk plasma just before and during disruptions across a wide range of disruption types [V.Riccardo et al., NF to be published] demonstrates that most discharges reach disruption with a small fraction of the full performance thermal energy. The exceptions are disruptions following VDEs and ITB collapses (which also have the shortest thermal quenches). This reduced thermal load considerably improves life expectancy of the ITER divertor and plasma-facing components. In addition, energy deposition has been observed outside the divertor [P.Andrew et al., EPS 2003, paper P1-108], potentially improving the scope for ITER divertor material options but with a possible impact that requires further experimental clarification on the current choice of a beryllium first wall. In fast current quench disruptions, the electromechanical load due to the induced currents represents one of the most severe design conditions for in-vessel components. Based on data from JET [V.Riccardo et al., PPCF, submitted] and most other tokamaks [M.Sugihara et al. this conf.] the minimum linear decay time normalised to the plasma cross-section extrapolates to a 40 ms disruption for ITER. Contrary to expectations, the quench rate of high and low thermal energy disruptions does not appear to vary substantially.

6.4 Edge Localised Modes

Assuming that large Type I ELMs will have to be tolerated, and extrapolating current ELM data to ITER, expected divertor target erosion rates are still too high. However, the improved JET database now estimates the expected ELM size to be only about a factor of 2 above the limit for target ablation (C or W targets). This is to be compared to a pre-2002 prediction of a factor of 5. In many cases, Type I ELMs on JET are also associated with rapid displacements of the divertor strike points, often over several cm. This is of potential importance for ITER with regard to power deposition. Very recent measurements in the far SOL of JET [Pitts et al., to be submitted - PRL] provide strong evidence that ELM ion energies remain high near the wall radius. This has implications both for the energy density on the first wall during ELMs but also for the degree to which ELMs may be tolerated in a reactor with a high Z wall. It has been found, moreover, that although ELM energy deposition becomes more balanced between inner and outer divertor targets at high I_p , larger ELMs tend to deposit increasingly lower fractions (as little as 50%) of the pedestal energy in the divertor region [T.Eich et al., PSI 2003; to be published in J.Nucl Mater], the rest being intercepted by main chamber wall surfaces.

High I_p , high input power operation at JET has also recently produced examples of ELMs with low frequency (~4 Hz), each carrying 1 MJ of plasma stored energy. There is evidence for target ablation and strong impurity influxes during these events (Fig. 5a/b), demonstrating a unique JET capability to explore ITER relevant ELM induced erosion. In many cases, large Type I ELMs are also associated with rapid displacements of the divertor strike points, often over several cm. This is of potential importance for ITER with regard to power dispersal. Improved measurements together with modelling on JET, support the conjecture that these jumps may be due to the peeling off of a current carrying plasma layer during the ELM [E.Solano et al., this conf.].

Using configurations optimised for pedestal and divertor diagnosis (so-called DOC-L, DOC-U), a large database describing Type I ELM behaviour and the H-mode pedestal profiles has been compiled. At high δ and q_{95} , so-called 'convective' Type I ELMs (i.e. ELMs for which the decrease in the pedestal pressure due to the ELM is mainly due to a decrease in temperature) have been found in JET at low pedestal collisionality. If such a regime were also found in ITER, extrapolated ELM target power densities would be within tolerable limits. [A.Loarte et al., Phys. Plasmas 11 (2004) 2668].

Regimes with intrinsically small ELMs have been pursued via dimensionless similarity studies with both Alcator C-Mod (EDA H-mode) and ASDEX-U (Type II). Despite considerable effort, it has not yet been possible on JET to reproduce the EDA H-Mode. On the contrary, by operating at low I_p (1.2MA) in order to obtain high poloidal beta ($\beta_p > 1.6$), as originally developed on JT-60U, and using a quasi-double-null configuration, pure Type II ELMs have been obtained for the first time on JET, albeit at rather high values for $q_{95}=6-7$ and high $v^*=(10-12)\times v^*_{ITER}$. To test this regime at higher currents, power levels are needed exceeding current heating capabilities at JET. [J.Stober et al., this conf.; Saibene et al., EPS 2004]

Active moderation of ELMs by N_2 impurity seeding in plasmas at $I_p/B_t = 2.5\text{MA}/2\text{T}$ has successfully demonstrated an integrated operational regime using nitrogen seeding by raising the radiated power fraction up to 95% resulting in a Type III H-mode. Confinement is reduced by about 20% but extrapolation of this regime to ITER show that nevertheless $Q=10$ is possible, by running ITER at 17MA [J.Rapp et al., Nucl. Fus., **44**, 312-319 (2004)]. Sustained steady conditions up to $H_{98}\sim 1$, $\beta_N=1.8-2.0$ for $n/n_{GW}=1-1.1$ have been separately achieved through argon seeding of Type I ELMing regimes under dual real-time feedback control, using majority and impurity gas inputs as actuators. [P.Dumortier et al., EPS 2004, P.Monier-Garbet et al., this conf.]

7. Heating and Current Drive

7.1 Plasma rotation

Plasma rotation is important for MHD stability and transport. In ITER, the external momentum input will be substantially lower than in most present day experiments. It is thus of considerable interest that significant co-current rotation has been observed in ICRF heated plasmas with negligible external momentum (heating with symmetric phasing of the antennas). Especially in view of the similarity with a burning plasma sustained by alpha particles, i.e. a strong presence of fast ions and no external momentum injection. In fact, fast ions have been suggested as a source for the observed rotation [Perkins F.W. et al. Phys. Plasmas 8, 2181 (2001)]. Their effect on plasma rotation has also been demonstrated recently in JET experiments with directed ICRF waves [L.-G. Eriksson et al., PRL 92 (2004) 235001]. However, an analysis of the JET results indicate that the effect of the fast ions is overlaid on an, as yet, unidentified mechanism responsible for the bulk of the observed co-current rotation. Nevertheless, the JET experiments showed that it is possible, at least partly, to control the rotation profile with the propagation direction of the ICRF waves.

7.2 ICRF heating scenarios

Various ICRF scenarios have been studied and/or further optimised to increase our understanding of the ICRF physics relevant to ITER.

Fundamental T heating in a trace Tritium plasma has required JET to operate at the lowest frequency (23 MHz) and the highest fields (4T). With 1.5 MW of ICRF energetic T tails of 80 to 120 keV near the optimum fusion cross-section have been produced, increasing the neutron emission by three orders of magnitude. Second harmonic T was shown to be better suited to a plasma with higher T concentrations while the presence of impurities (C or Be) make minority heating of D in H almost impossible since the C^{6+} impurity, which has the same cyclotron layer as D, influences wave propagation like a much higher equivalent D concentration and directly leads into the mode conversion regime. [P.Lamalle et al., this conf.].

Minority heating of 3He in H was studied with 5MW of ICRF (3He concentrations varied from 1% to 10%), and is found to be a suitable candidate for the non-activated phase of ITER. The transition from minority heating (3He effective temperature of 100 keV, T_e up to 6 keV) to mode conversion heating (electron heating, T_e up to 8 keV) was sudden and reproducibly near a 3He concentration of 2 %. In the mode conversion regime, with directed waves, no CD effects were observed. [P. Lamalle et al, this conf.].

An experiment to study pT fusion reactions ($p+T \rightarrow ^4He+n$) has been performed during the TTE campaign at JET. Hydrogen minority heating was used to produce energetic proton tails, causing neutron emission from the pT fusion reaction. The observed neutron yield depends on plasma parameters as expected, apart from some discrepancies at very low tritium concentration. The results show the importance of taking into account the neutron contribution from pT fusion reactions while analysing neutron measurements in purely RF heated tritiated plasmas. [M.Santala et al., EPS 2004]

7.3 ICRH Conjugate T-matching

The use of 3 dB couplers allow a reliable operation of ICRF generators in the presence of strong load variations such as large sawteeth and ELMs. [J.-M.Noterdaeme et al., SOFT 2004], and will be implemented on half of the JET antennas in 2005. Conjugate T-matching is another method that promises to maintain the power to the plasma even during the ELM coupling transients and is at the basis of the JET-EP antenna concept [F.Durodie et al., SOFT 2004]. Proof of principle tests using a temporary set-up connecting two adjacent straps of one of the existing A2 antennas in an external conjugate T-configuration were done in an ELMy H-Mode with ITER like plasma shape ($\delta^{up} \sim 0.48$, $\delta^{low} \sim 0.35$) at $I_p/B_t = 2.5MA/2.7T$, heated with $\sim 15MW$ of NBI, resulting in large Type I ELMs. The antenna straps in the conjugate T configuration, fed by one generator with 2MW output, coupled - without pushing the system to its limits - immediately a steady power of up to 800kW for a flattop time of 5s, while the traditional A2 antennas had a very erratic coupling behaviour to the same plasma. These results are in good agreement with simulations. [I. Monakhov et al., SOFT 2004].

7.4 LHCD Coupling

LHCD has been a key tool in the further development of ITB plasmas on JET, and substantial progress has been made in view of ITER. Using a recently modified gas pipe to optimise the gas flow near the launcher, thereby improving the deposition of the gas in the region magnetically connected to the LH launcher, up to 2.5 MW of LH power was coupled at an ITER relevant distance of 10 cm with a reflection coefficient $< 8\%$, even during large amplitude Type I ELMs. On ELMs with smaller amplitude, up to 3MW of LH power has been coupled at a plasma distance of 11cm. These results have to be compared to 1MW of LH power coupled without gas injection. This has been obtained with D_2 injection, therefore rendering the use of CD_4 (which is questionable in combination with T because of concerns of T co-deposition) no longer mandatory for good coupling results [J.Mailloux et al., A. Ekedahl EPS 2004; PRL, in print]

8. Diagnostics

8.1 Edge diagnostics

Particular efforts have been devoted to improve the spatial resolution of the various measurements in the plasma core, doubling the ECE channels [E. De La Luna et al., accepted for Rev Sci. Inst. 75 (2004)] and increasing the accuracy of the active spectroscopy by increasing the energy of the neutral injector used for the MSE diagnostic from 80keV to 130keV. Particular attention has also been devoted to the edge, which in general is a

difficult plasma region for measurements. The Li beam diagnostic has been enhanced increasing the energy of the beam atoms from 30 to 60 keV and the current from 0.2mA to 1mA [A.Korotkov et al., Rev. Sci. Instr. 75, 2590-2602 (2004)], enhancing the penetration by at least 50% in ELMy H-Mode plasmas, and allowing the measurement of the electron profile in the region of strong gradients with a spatial resolution of 1 cm and an absolute accuracy of 3%. Both the response times of the fast digitiser and the detectors of the edge LIDAR system have been shortened, resulting in a doubling of the global spatial resolution (from 12cm to 6cm) [M.Kempenaars et al, Rev. Sci. Instr. 75, (oct 2004)]. Together with the development of special plasma configurations (DOC-L and DOC-U) which are designed to maximise the number of simultaneous plasma edge measurements, these enhancements have allowed a much more detailed study of the gradients of electron temperature and density in the edge, and a better documentation of the nature of the ELMs. (See Section 6.4). [A.Loarte et al., this conf.].

8.2 Burning Plasma Diagnostics

Significant progress has been obtained in the measurement of the 3.5MeV alphas and the 14MeV neutrons, and a direct measurement of all products of the D-T reaction in JET is now possible. Gamma ray spectroscopy now provides almost routinely the spatial distributions of the fast particles (fast D and He ions accelerated by ICRF, or 3.5MeV He particles from the fusion reaction). The technique is based on the detection of gamma rays from the nuclear reactions ${}^9\text{Be}(\alpha, n\gamma){}^{12}\text{C}$ and ${}^{12}\text{C}(d, p\gamma){}^{13}\text{C}$ which both have a high energy threshold for the alpha ($E > 1.7\text{MeV}$) resp. D ($E > 0.8\text{MeV}$) particle involved. The gamma rays are sufficiently separated in energy (4.44MeV, resp. 3.01MeV) to allow a good discrimination between both, thus allowing a simultaneous measurement (Fig. 6). Moreover, by observing the time dependence of the gamma ray emissions, the confinement of the fast alphas could be directly observed for the first time in a tokamak in various plasma regimes (See Section 5.1). The technique has been extended to the detection of fast ${}^3\text{He}$ and H particles, using resp. the reactions ${}^{12}\text{C}({}^3\text{He}, p\gamma){}^{14}\text{N}$ (gamma emission at 4.78MeV) and ${}^{12}\text{C}(p, p'\gamma){}^{12}\text{C}$ (gamma emission at 4.44 MeV). Further development of the gamma-ray diagnostics towards a higher time resolution and operations with neutron filters in the presence of large fluxes of DT neutrons (as will be required for ITER) is being considered for future JET operations.

For the study of lost fast particles, a new diagnostic has been developed based on the activation of suitable samples (depending on the energy of fast alphas to be detected, fluor-titanium compounds), and has allowed to confirm the theoretically predicted dependency of the fast losses on the poloidal angle. [G. Bonheure et al., Rev.Sci Instr. 75, 3540 (2004)]. The technique has the potential to discriminate between the losses of various fast particles, and will be further pursued in future campaigns.

The Magnetic Proton recoil Spectrometer has been further refined to also allow absolute measurements of the total 14MeV neutron yield. The results of the spectrometer are in agreement with the other two independent neutron measurements at JET (neutron cameras and the delayed emission samples), and JET is now the only machine in the world having 3 independent measurements of the total neutron yield. Detailed tritium transport studies have been performed with the JET horizontal and vertical neutron cameras and new ITER relevant compact detectors (NE213 14 MeV neutron spectrometer [A.Zimbal et al., Rev.Sci.Instr. 75, 3553 (2004)] and Carbon Vapour Deposited (CVD) diamond counters [M.Angelone et al., EFDA JET Report PR(04)10 (2004); Rev.Sci. Instr. accept. for publ.]) have been successfully tested, for the first time in a tokamak environment, and offer excellent prospects for use on ITER.

Major progress has been obtained in determining the plasma isotopic composition. The tritium content of the plasma was measured for the first time during TTE using a Neutral Particle Analyser (NPA), especially designed for the determination of the isotopic composition by detecting simultaneously the neutral fluxes of all hydrogen isotopes leaving the plasma at various energies and therefore from different radial positions. [M.Mironov et al. EPS 2004, paper P1-149]. This diagnostic is particularly effective for neutrals born in the outer regions of the plasma, where it complements the core measurements of the neutron cameras.

The study of Alfvén Cascades excited with fast ions in reversed magnetic shear plasmas has been greatly facilitated using a novel microwave interferometry technique. The technique measures the density perturbations associated with ACs. This technique is much more sensitive to their presence than detection with pickup coils, because the density perturbation contributes twice along the path of the microwaves through the plasma, while external pickup coils detects only those modes for which the (low amplitude) tail can reach the coil in the plasma edge. An illustration of the results obtained with the new technique clearly shows the unprecedented frequency and time resolution (detection of mode numbers up to $n=16$) compared to the conventional technique [S.Sharapov et al., PRL 93, 165001/1-4].

9 Conclusion / Progress towards ITER

In the past 2 years, JET has continued to contribute to all aspects of plasma scenario development for ITER.

High density and high confinement operation in ELMy H-Mode is confirmed at or above the normalised parameters foreseen for the ITER operating point ($H_{98(y,2)} \sim 1$, $n/n_{GW} \sim 1$, $\beta_N > 1.8$ at $q_{95} \sim 3$), increasing further the confidence in the Q=10 reference scenario for ITER. Furthermore, the scaling of the ELMy H-Mode with β_N could be more favourable than predicted by the IPB98(y,2) scaling expression, and this would imply a significant improvement in fusion power production and Q at higher values of β_N (> 1.8). Experimental results indicate an increased density peaking at lower collisionality, consistent with theory, which, if confirmed at high β_N , low ρ^* and possibly with more electron heating, would also impact on fusion power production. The removal of the septum from the divertor has no detrimental effects on the L-H power threshold and plasma performance. ICCD control of fast particle stabilised sawteeth has been demonstrated for the first time; the underlying NTM and sawtooth physics is being refined in view of the need for NTM control on ITER.

At high-density type-I ELMy H-modes show trends that would lead to marginally acceptable ELMs on ITER; a regime at high d and q_{95} but nevertheless low pedestal collisionality, shows convective Type-I ELMs which would be tolerable on ITER. Quiescent edge or small (type II) ELM regimes are so far difficult to reproduce on JET, which could be an indication of an unfavourable ρ^* , v^* dependence; e.g. a Type II ELM regime has been produced, but under very restrictive conditions, at low current (1.2 MA), high heating power, high β_p and high shear resulting from quasi double null and high q_{95} operation. Type III ELMy operation with radiation fractions up to 95% has been demonstrated by seeding of N_2 in H-modes and could extrapolate to $Q=10$ ITER operation, albeit at high current (17 MA). The mitigation of Type-I ELMs nevertheless remains a challenge and appropriate techniques will need to be developed (pellets, magnetic perturbation coils etc.).

Plasma performances with Internal Transport Barriers (ITB) progressed considerably, with operation at either central densities close the Greenwald density or/and low toroidal rotation or/and high triangularity, at b_N up to 2.7. The first demonstrations of simultaneous real time control of safety factor and temperature profiles have been achieved in ITB plasmas. Highly non-inductive current drive reversed shear 3T/1.8 MA plasmas have been optimised for long pulse operation with a duration of up to 20s. Extrapolation to ITER of RWM damping experiments in ITB plasmas shows that a low bulk plasma rotation should be sufficient to stabilise RWMs; nevertheless, implementation of means to control RWMs on ITER seems prudent. High $\beta_N \sim 2.8$ operation of hybrid modes has been obtained at 1.7T/1.4MA. However at lower ρ^* values (3.1T/2MA and 3.4T/2.8MA) β_N appears to be limited by lack of heating power. Hybrid modes have also been obtained with dominant RF heating. For ITER, the ρ^* , v^* , β_N ... scaling of ITB and hybrid modes needs to be determined; this requires further experiments with higher heating power.

Trace Tritium Experiments (TTE) yielded valuable information on particle transport, indicating anomalous values of particle diffusion and convection in H-mode, reducing to neo-classical levels in high density, low q plasmas and in ITBs. Scaling of T transport with ρ^* , v^* and β_N has been investigated.

Minority heating of ^3He in H was studied with 5MW of ICRF and is found to be a suitable candidate for the non-activated phase of ITER. In ELMy H-modes, 2-3 MW of LHCD have been coupled at ITER-relevant plasma distances of 10-11cm. Proof of principle tests of ICRH conjugate T-matching have been successfully conducted in Type I ELMy plasmas.

Operation during the last campaigns resulted in reduced retention of D (as seen from post-mortem tile analysis) and T (as seen from post TTE clean-up). This is likely related to the more recent tendency for vertical target operation in the divertor (compared to horizontal targets in DTE1) and/or lower (ITER-like) vessel temperatures. Experiments confirm that erosion occurs predominantly on main chamber surfaces implying that an all metallic wall on ITER could be beneficial in reducing T-retention, although the consequences of erosion for the lifetime of the ITER Be first wall need to be assessed. The divertor cannot, however, be excluded as a source of erosion and carbon targets on ITER are still likely to result in significant T-retention.

Improved measurements are showing that for large Type I ELMs, only $\sim 50\%$ of the plasma energy loss reaches the divertor. Likewise, it is becoming clear that energy flow to the divertor during most disruptions occurs over slow enough timescales and large enough area (5-10 times the normal wetted area) to provide a favourable extrapolation to ITER. Transient power deposition is nevertheless likely to be more challenging for the metallic first wall.

Progress in burning plasma physics has been made possible by the further development of alpha simulation techniques and burning plasma diagnostics. In particular, the first direct observations of alpha particle slowing down and alpha particle tomography have been made possible by γ spectroscopy; application on ITER requires appropriate neutron shielding techniques to be developed. Measurements of Alfvén cascades have been improved dramatically by a new interferometric technique allowing high n-mode observation. Advances in the use of neutron cameras, neutron spectrometry and neutron counting detectors provided essential inputs to the design of neutron diagnostics in ITER.

Acknowledgements

All those who have been involved in the preparation of this paper are gratefully acknowledged, with special thanks to Y.Andrew, R.Buttery, M.Gryaznevich, X.Litaudon, P.Mantica, A.Murari, D.McDonald, J-M. Noterdaeme, R.Pitts, S.Sharapov, M.Watkins and K.D.Zastrow. This work has been conducted under the European Fusion Development Agreement.

Figure 1 is a plot of normalized beta_N versus normalized pressure gradient $\rho^* \times 10^{-3}$ for $q_{95} = 4$. The plot shows experimental data points for various tokamak configurations, categorized into 'Power limited' and 'MHD limited' regions. The 'Power limited' region is shaded gray and contains data points for RF-heated hybrid scenarios (circles and triangles) and JET (green circles). The 'MHD limited' region is shaded red and contains data points for AUG (blue circles) and DIII-D (yellow triangles). The plot also shows theoretical limits for ITER and JET. The y-axis is β_N (0 to 3) and the x-axis is $\rho^* \times 10^{-3}$ (1 to 10).

As β Increases, Performance Increases more Favorably than the Conventional Prediction

Projected Fusion Performance

β_N

● = JET
■ = DIII-D

Conventional prediction

ITER shape and parameters are utilized

β_N	Projected Fusion Performance (JET)	Projected Fusion Performance (DIII-D)
0.8	-	3.5
1.0	7.0	-
1.1	-	5.5
1.6	-	9.5
1.8	12.5	-
2.1	18.0	-
2.3	-	13.0

Fig.3 Increase in fusion power expected for ITER from the β independence of ELMy H-Mode confinement, as observed on JET and DIII-D, in contrast to the nearly inverse β_N dependence of the IPB98(y,2) scaling. The prediction for the fusion amplification Q in the ITER reference scenario on the basis of IPB98(y,2) is shown by the full line. Extrapolations from JET(bullets) and DIII-D data (squares) show an increase for the Q value of ITER for $\beta_N > 2$.

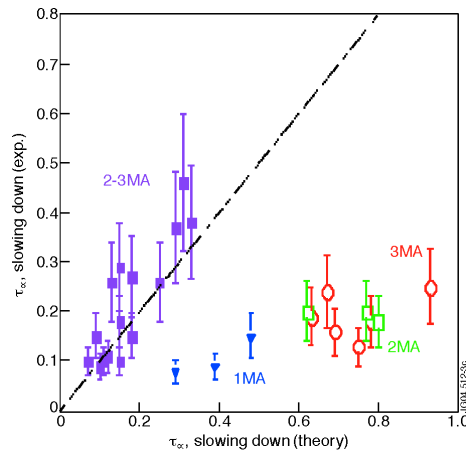


Fig 4. Experimental fast alpha slowing down times in JET and comparison with classical slowing down. Data are taken at different currents from reversed shear discharges with current hole (open symbols) and without current hole (full symbols). High current discharges ($I_p > 2\text{MA}$) without current hole follow nicely the theoretical predictions. Data from discharges at low current ($I_p < 1\text{MA}$) or with a current hole show ~ 5 times smaller slowing down times, indicative for degraded alpha particle confinement.

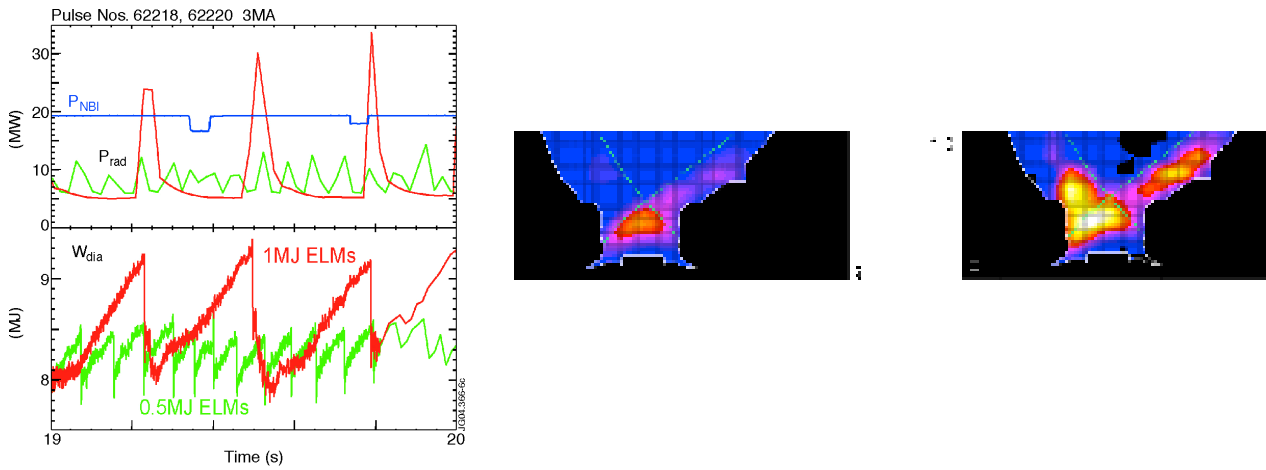


Fig 5a (left). Illustration of the effect of large ELMs ($\Delta W_{\text{dia}} \sim 1\text{MJ}$) in JET (bottom figure). Radiation peaks at the crashes of these large ELMs are observed (upper figure). A comparison is shown with the effect of smaller amplitude ELMs ($\Delta W_{\text{dia}} \sim 0.5\text{MJ}$).
 Fig 5b (right). A 2D bolometric reconstruction before (left part) and after (right part) 1MJ ELMs, showing the dramatic increase in radiation.

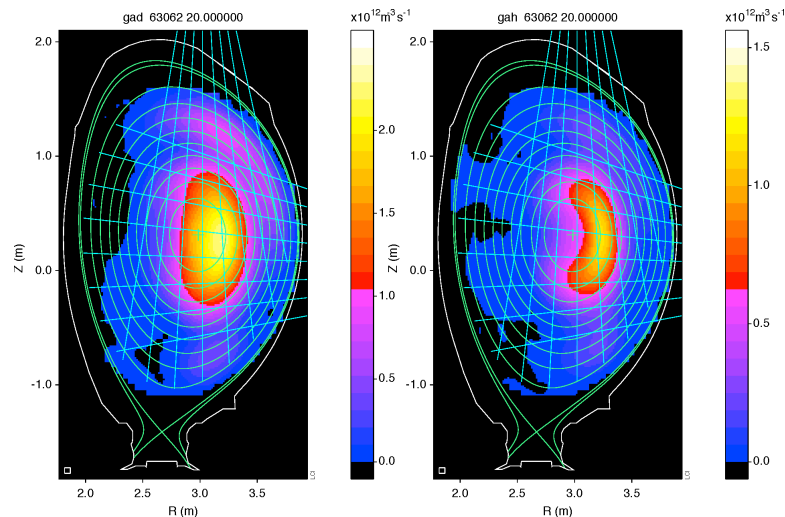


Fig 6. Tomographic reconstruction of fast D ions (left) and fast alpha particle (right) measured simultaneously in a discharge with alpha and (parasitic) D ion acceleration with ICRF